13th World Conference on Earthquake Engineering
Vancouver, B.C., Canada
August 1-6, 2004
Paper No. 1442

SEISMIC VULNERABILITY ASSESSMENT OF THE SANTA MARIA HOSPITAL, IN LISBON

Jorge PROENÇA[1], Carlos Sousa OLIVEIRA[2] and João Pacheco ALMEIDA[3]

SUMMARY

The Santa Maria Hospital, in Lisbon, is an example of a large, early reinforced concrete, important building complex, built in the early 1950s, before Portuguese structural codes considered earthquake-resistant design related issues.
The seismic vulnerability assessment stages comprised on-site inspection, documental collection, ambient vibration modal identification, development of numerical models for seismic structural vulnerability assessment and seismic vulnerability assessment of non-structural components such as basic facilities, equipment and architectural components.
The conclusions express the expected structural and non-structural seismic performance, and point to damage reduction guidelines, aimed at the structural retrofit strategy, as well as to the improvement of the connections of some basic facilities components.

INTRODUCTION

The Santa Maria Hospital building complex, shown in Figure 1, consists of 47 cast-in-situ reinforced concrete frame building blocks, 1 to 11 storeys high, separated by expansion joints. This Hospital has a total area of 120 000 m^2, presently with 1560 internment beds, being situated in Lisbon, in the Portuguese highest seismic risk zone. The building design and construction started in the late 1930s and ended in 1953, before earthquake-resistant design clauses were included in the Portuguese structural design codes.

In 2002 DGIES – Direcção Geral de Instalações e Equipamentos de Saúde, from the Portuguese Health Ministry, asked ICIST – Instituto de Engenharia de Estruturas, Território e Construção – to assess the seismic vulnerability of the Santa Maria Hospital. This study was finished in April 2003, Oliveira [1].

The seismic vulnerability assessment stages consisted of:
- documental collection;
- on-site inspection of structural and non-structural components;
- ambient vibration modal identification for a significant number of building blocks;

[1] Assistant Professor, DECivil, ICIST/IST, Av. Rovisco Pais, Nº 1, 1049-001, Lisbon, Portugal
[2] Full Professor, DECivil, ICIST/IST, Av. Rovisco Pais, Nº 1, 1049-001, Lisbon, Portugal
[3] MSc scholarship student, DECivil, ICIST/IST, Av. Rovisco Pais, Nº 1, 1049-001, Lisbon, Portugal

- seismic structural vulnerability assessment for some of the most representative building blocks;
- seismic vulnerability assessment of non-structural components.

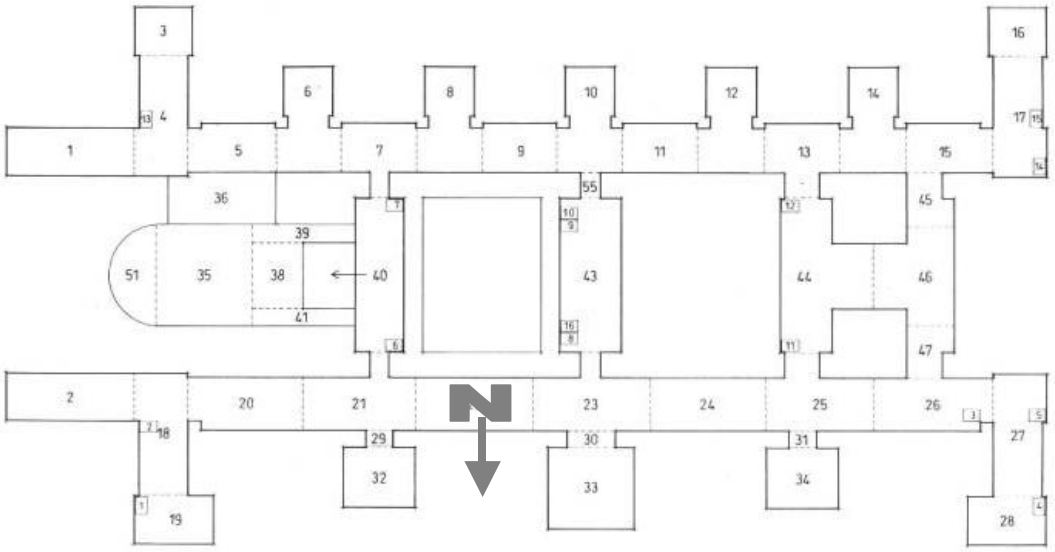

Figure 1: General plan and identification of building blocks.

This paper focuses on the (structural and non-structural) seismic vulnerability assessment stages, which are dealt with in two different sections, preceded by a brief presentation of the modal identification stages. The following section summons up the results of the documental collection and preliminary inspection stages.

Documental Collection and Preliminary Inspection

The Santa Maria Hospital presents two main, E-W oriented wings, with three transversal connection building blocks as shown in Figure 1. The majority of the building blocks are 10-storeys high, whereas the corner blocks (#3-4, #16-17, #18-91 and #27-28) have an extra storey and every two of these corner blocks have a 150m^3 reinforced concrete water tank on the roof. The prevailing structural solution consists of cast-in-situ plane RC frames with cast-in-situ ribbed slabs (the ribs being set perpendicular to the frame beams).

Despite being aware of the "earthquake peril", the structural designer did not consider earthquake loads at the design stage because he considered that the RC frame structure had an intrinsic lateral force resisting strength that would suffice in the event of an earthquake. The building blocks were originally designed for relatively intense wind pressures of 1,47 kN/m^2 on the exposed facades, leading to the RC frames being predominantly set perpendicular to these. The building blocks in the two main wings have their frames in the N-S direction, with the exception of the corner blocks that present frames in both horizontal directions. The transversal connection blocks have their frames in the E-W direction.

The reinforced concrete elements' detailing is characterized by low ductility, as can be expected by the use of smooth reinforcing bars, large stirrup spacing in the columns and outdated detailing rules. The average concrete compressive strength, as determined from a group of drilled concrete-core samples, was 20 MPa for beam and column elements. The steel reinforcing bars yielding stress varied, according to the bar diameters, from 299 MPa to 358 MPa, with and average value of 307 MPa.

In spite of not having been considered as a part of the (lateral or vertical) structural load-resisting system, the building blocks have structurally non-negligible internal and external masonry walls. The exterior masonry walls contain rubble stone blocks in the lower storeys and dense ceramic bricks in the upper storeys.

MODAL IDENTIFICATION

The lateral load structural behaviour of the building blocks is highly dependent on the effectiveness of the separation joints, as well as on the stiffness and strength contribution of the masonry wall panels. Considering these uncertainties and prior to the development of refined numerical models, the modal identification stage was undertaken. The modal identification stage was subdivided into the *simplified*[4] modal identification of fourteen different building blocks, amongst which the building block #22, and the *complete*[5] modal identification of building block #4 (one of the corner building blocks).

The *simplified* modal identification is based on the assumption that ambient vibration excitation can be considered equivalent to a white-noise process, in which the peaks of the response power spectral density (or of its Fourier transform) correspond to the modal frequencies. Figure 2 depicts the normalized Y-direction (N-S) acceleration power spectra for ambient vibration records collected in building blocks #8, 9, 10, 16, 17 and 43.

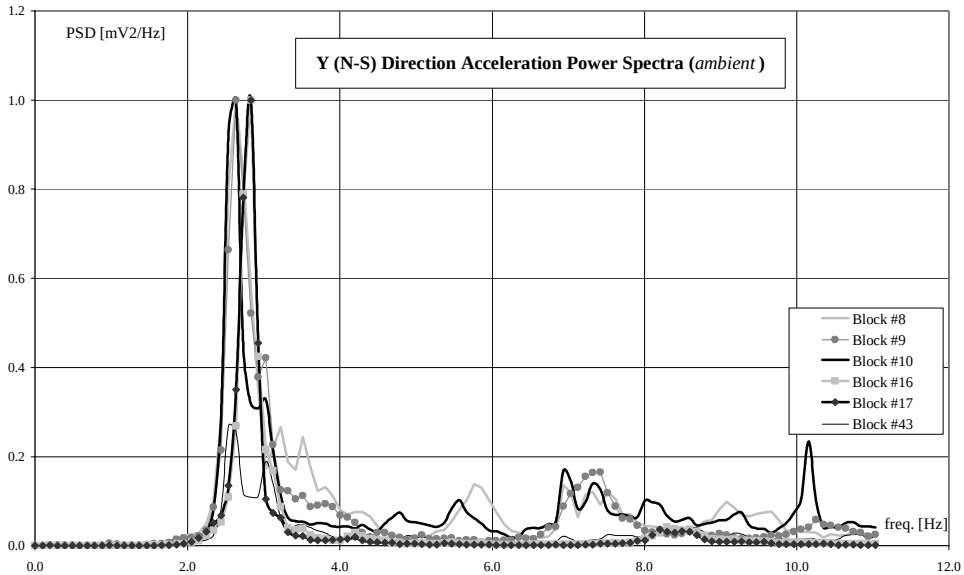

Figure 2: Normalized ambient vibration acceleration power spectrum for building blocks #8, 9, 10, 16, 17 and 43 (Y-direction).

These modal identification results clearly point out to a unified behaviour of the building blocks with a fundamental frequency value of 2.4-2.8 Hz for X (E-W) direction and 2.4-2.8 Hz for Y (N-S) direction.

---

[4] The *simplified* modal identification is aimed only at the identification of the fundamental frequencies, which can be accomplished by the collection of ambient vibration records at a single storey, generally the highest one.

[5] The *complete* modal identification is aimed at the identification of modal frequencies and modal shapes of a given building structure, requiring intensive and lengthy instrumentation of all building storeys and the collection of synchronized ambient vibration records.

The *complete* modal identification of building block #4 was performed according to the BFD – Basic Frequency Domain – algorithm, which assumes that:

$$\frac{\ddot{Y}_a(\omega_j)}{\ddot{Y}_b(\omega_j)} \approx \frac{\omega_j^2 \Phi_{a,j} \cdot H_j(\omega) \cdot Q_j(\omega)}{\omega_j^2 \Phi_{b,j} \cdot H_j(\omega) \cdot Q_j(\omega)} = \frac{\Phi_{a,j}}{\Phi_{b,j}}$$

where:

$\ddot{Y}_a(\omega_j)$ and $\ddot{Y}_b(\omega_j)$ stand for the Fourier transforms of the ambient vibration acceleration records at levels (storeys) a and b.

$\Phi_{a,j}$ and $\Phi_{b,j}$ represent the j^{th} modal shape coefficients at storeys a and b.

ω_j is the (angular) modal frequency of mode j

$Q_j(\omega)$ is the Fourier transform of the j^{th} mode modal force

$H_j(\omega)$ is the (SDOF) force-to-displacement transfer function for mode j

The former equation states that the modal shape coefficients at storeys a and b can simply be assessed through the computation of the correspondent ratio of the acceleration Fourier transform ordinates for modal frequency ω_j. The j^{th} modal frequency can, in turn, be identified through the peaks of the Fourier transforms of (response) acceleration records at any of the storeys, provided that neither of these is a nodal point of the correspondent modal shape. Figure 3 depicts the fundamental mode shapes in the X and Y direction for building block #4.

Storey	Φ_{1X}	Φ_{1Y}
10	1	1
9	0.906	0.953
8	0.776	0.91
7	0.674	0.819
6	0.537	0.688
5	0.415	0.555
4	0.307	0.428
3	0.225	0.291
2	0.114	0.128
1	0.052	0.054
0	0	0

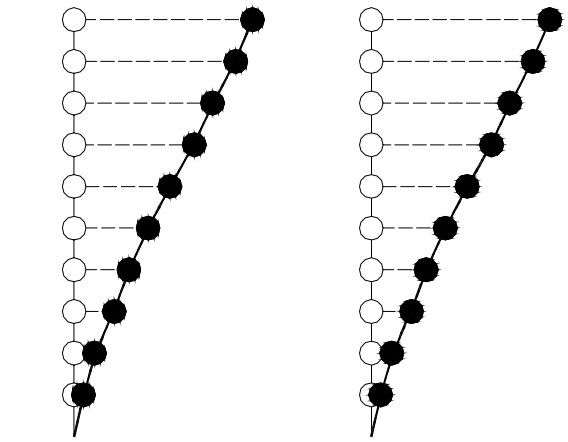

Figure 3: Fundamental mode shapes for building block #4.

One of the most striking results is that the maximum inter-storey drift occurs within intermediate storeys, leading to higher demands on the (RC and masonry) elements in-between these storeys.

The modal identification stages stressed out the stiffening contribution of the masonry infill panels – without which the fundamental frequencies would be much lower – as well as the strong interdependency of the dynamic behaviour presented by neighbouring buildings blocks.

STRUCTURAL VULNERABILITY ASSESSMENT

The seismic structural vulnerability assessment stages comprised the development of linear dynamic and non-linear static models, respectively for blocks #4 and #22, considered amongst the most representative buildings blocks.

Building Block #4

Structural vulnerability assessment of building block #4 was mainly conducted by means of a linear dynamic analysis with the following two distinct, "extreme", models: model 1 – model with the stiffening effect of external and internal masonry walls; and model 2 – bare frame model. Irrespectively of the model, the results expressed both by the inter-storey drift and by the relevant stresses in some of the columns, led to the preliminary conclusion that the structure is over-designed. This conclusion relies heavily on the assumed shear reduction factor (q=2) and on the assumption, dispelled by the analysis of building block #22, that the stress and deformation distribution should not significantly change in the non-linear range.

Building Block #22

Structural vulnerability assessment of building block #22 was conducted through a more informative displacement-based design approach. The assessment stages comprised initial linear model, non-linear model and actions, and pushover analysis, which are described separately in the following sub-sections.

Initial Linear Model

The building block number 22 is located in the north wing of the Hospital, as shown in Figure 1. The structure consists of nine storeys with six 2D transverse RC frames with a spacing of approximately 5.75 m. The building plan is rectangular, 28.91 m by 12.65 m for the first 5 floors, with a setback of 4.31 m in the direction of the frames for the top storeys. The storey height varies between 3.0 m and 4.0 m. All the slabs are one-way, spanning between the frames (Figure 4).

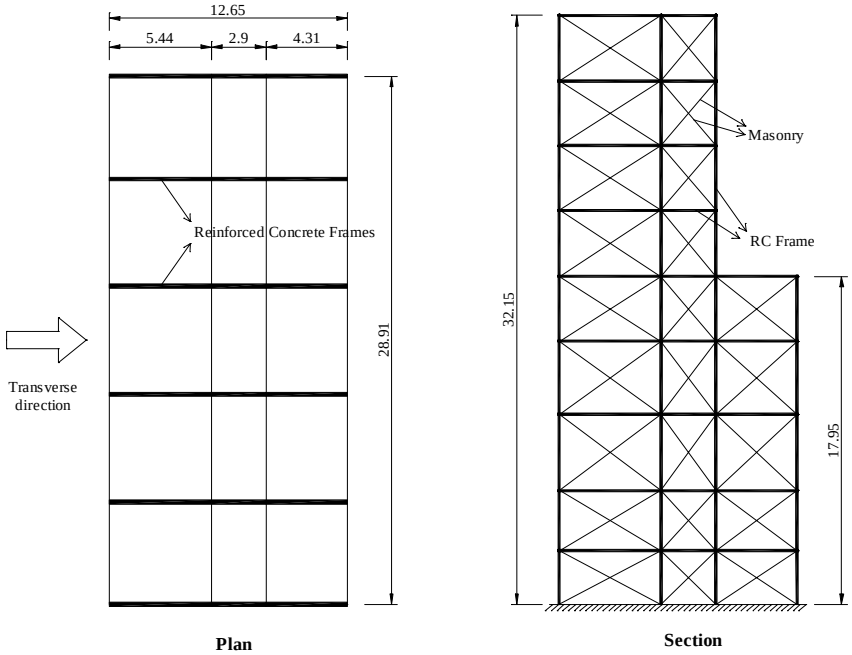

Figure 4: Block #22. Plan and side view.

The building was modelled using a 3D finite element model, with frame elements representing beams and columns. The external and internal masonry infill panels were also modelled using a pair of diagonal frame elements for each panel, the details of which are discussed later. The storey slabs were represented by equivalent beams and modelled as rigid diaphragms. The nonlinear static analysis requires the consideration of the actual force-deformation relationships for all sections, which, in this case, were based on the longitudinal reinforcements of the beams and columns, taken from the original design documentation. The numerical analyses (dynamic elastic and static inelastic) were carried out with SAP2000 Nonlinear, v.7.42, Computers and Structures Inc. [2].

The preliminary structural model consisted in a bare RC frame without the consideration of the stiffening effect of the masonry infills, leading to fundamental period values approximately 4 times the experimental values. In face of such a discrepancy it was decided that the numerical model should include the stiffening effect of these non-structural elements.

On-site inspection led to the discrimination of two different types of masonry materials and modelling rules. In the longitudinal direction of the first four storeys, the masonry panels comprise rubble stone blocks (E=5 GPa, fw=5 MPa, width=0.5 m), having been modelled with struts whose widths are 15% of the diagonal length. For the remaining storeys in this direction, as well as for all the panels in the transverse direction, the solid brick blocks masonry panels (E=3 GPa, fw=2.5 MPa, widths varying from 0.20 m, transversal, to 0.30 m, average longitudinal) were modelled through diagonal struts with a cross-section area equivalent to 20 % of the diagonal length of the respective panel.

The gravity loads considered in the analysis were: the dead loads for the beams, columns, slabs (with finishes) and walls (exterior and interior, based on the previously presented geometric dimensions). The dead loads due to partition walls on the slabs were of 2.0 kN/m2 and the live load was of 3.0 kN/m2, as prescribed for hospitals in Portuguese National Codes, MHOPT [3], reduced by a factor of 0.4 according to the same Code.

After the inclusion of the masonry infill stiffening effect, the numerical model yielded fundamental frequency values in close agreement with the experimentally determined results.

Nonlinear Model And Actions

The structural model referred so far had to be further refined in order to perform a nonlinear static (pushover) analysis, performed according to the Capacity Spectrum Method (CSM), as proposed by Applied Technology Council [4].

A pushover analysis model requires a series of hinges to account for the nonlinear behaviour of the various structural elements, which, in this case, are the RC beams and columns and the masonry elements. SAP2000 generates the hinges for the beam and column elements based on the existing reinforcement, on the material characteristics and on the provisions of both Applied Technology Council [4] and Building Seismic Safety Council [5]. The developed nonlinear structural model comprised PMM hinges (P - axial force; MM - bi-axial moments) for columns, M3 hinges (uniaxial moment) for beams, and P hinges (axial force) for the diagonal strut elements. Each beam was discretized into two finite elements due to the different reinforcement detailing near each column joint. Since the masonry tensile strength is negligible, only its compressive strength was considered. This parameter was computed by SAP2000 based on the cross-section area of the struts and on the allowable compressive stress. The ratio between the crushing and the cracking strengths was taken as 1.44, Pires [6]. Moreover, the crushing to cracking displacement ratio was taken as 1.5. Finally, to prevent numerical instabilities, this hinge was modified as shown in Figure 5, in such a way that the total compressive strength was equally divided into compressive and tensile zones.

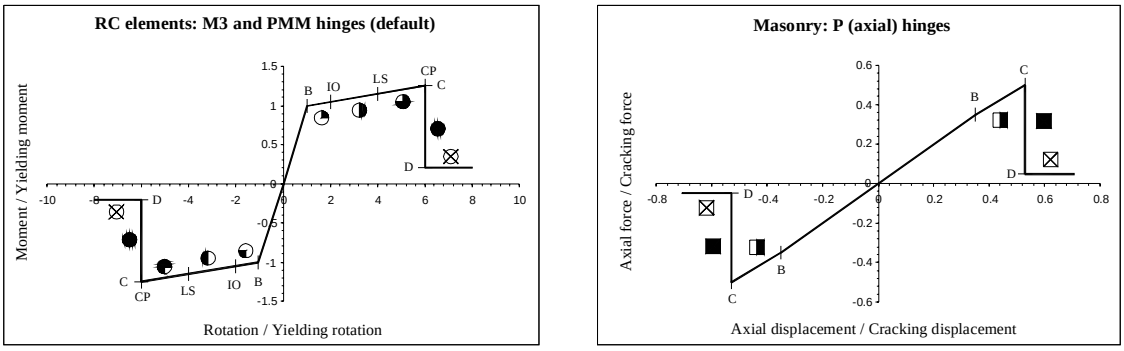

Figure 5: Concrete and masonry hinges (damage symbols).

Another important aspect in pushover analysis is the definition of the lateral loads, which, in this case, were considered proportional to the product of the storey masses by the fundamental elastic mode shape, assuming that this mode accurately describes the predominant response pattern of the structure. This approach is classified as Level 3, Applied Technology Council [4], and is recommended by the Applied Technology Council for buildings with fundamental mode periods up to about one second, such as the one under study.

The pushover analysis was carried out in two sequential stages: a first stage involving the application of the gravity loads; and a second stage in which the lateral loads were incrementally applied.

The seismic action was defined by the 5 % damping response spectrum in Eurocode 8, CEN [7], calibrated for the seismic zone of Lisbon. This response spectrum was further converted and fitted to the parameterised response spectrum that CSM methodology considers. The best fit values for the seismic coefficients were of Ca=0.2752 g and of Cv=4.048 m/s. The final response spectrum was represented in the Acceleration-Displacement Response Spectra (ADRS) format.

Pushover Analysis

Considering that in the longitudinal direction all building blocks, including # 22, should behave as a whole according to the conclusions of the modal identification stages, the pushover analysis was performed solely in the transversal direction (the direction of the main frames). The lateral force resisting system in the longitudinal direction should, presumably, rely on the corner blocks (#2, #18, #19, #27 and #28) whose frames are set in this direction.

The application of the gravity loads was performed in one single step due to the fact that none of the elements reached its yield or cracking strength.

The increments of the lateral load pattern led to the capacity curve presented in Figure 6 in terms of the base shear *vs* top storey displacement. This curve shows the cracking, yielding and crushing sequence of the various elements: as expected, the masonry elements are the first to crack – the three top storeys are the least affected, while the lower ones present generalized degradation. For increasing top displacement values, damage tends to concentrate at the intermediate levels (2nd, 3rd and 4th storeys), and, for a top displacement value of 6.2 cm, all struts at the 3rd storey reach their ultimate strength. Further loading increments result in the development of the well-known soft-storey phenomenon. Figure 6 also shows the damage inflicted both in the masonry and in the reinforced concrete elements at this step. More masonry elements at other levels have also reached their ultimate capacity at the onset of the soft-storey

mechanism. The damage in the RC elements is limited to yielding in some beams, especially those of the second and third levels.

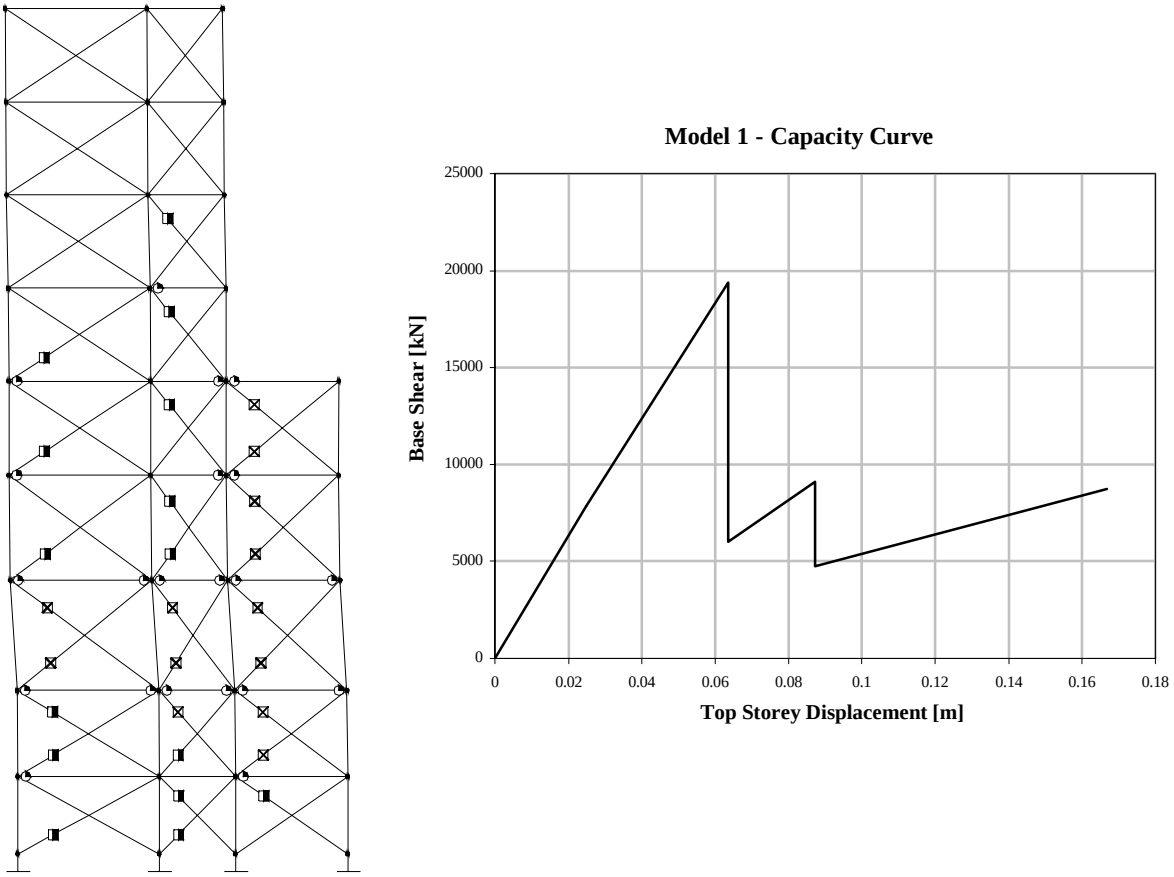

Figure 6: Model 1 –Layout of damage and capacity Curve at the instant of soft-storey formation (for damage symbols refer to Figure 5).

The formation of the soft storey is the first noteworthy drop in the lateral load system strength (marked with ○ in the 1st capacity curve of Figure 8) – the structure remains very stiff until the collapse of the intermediate storey infilled masonry set of walls. The model led to the formation of a weak 3rd storey, yet sensitivity analyses carried out afterwards showed that the soft-storey phenomenon could take place either in the 2nd or in the 4th levels, depending on the strength parameters of the diagonal struts. Crushing of these elements leads to a major transformation in the first mode shape and, consequently, also in the consistent lateral load pattern that should be applied to the structure to evaluate its performance. Consequently, this model was no longer valid for the subsequent structural assessment stages, and a new model had therefore to be developed.

The 2nd, damaged, model differed from the 1st model by the removal of all the elements that had attained their ultimate capacity (the diagonal masonry struts represented by ☒ in Figure 6) at the instant of the formation of the soft-storey.

According to Applied Technology Council [4], the final capacity curve can be determined combining different capacity curves at the displacement values corresponding to each strength degradation phenomenon, which is realistic provided that there is limited strength degradation. For the actual building and soft-storey phenomenon this assumption turns out to be unacceptable – the reasons for this statement

are explained latter in this paper. The combination of the former two capacity curves was performed according to a simplified (although coarse) process to take into account the expected building performance. The chosen adapted methodology is based on a rational interpretation of how the several (in this case, only two) capacity curves can be combined to obtain more precise results.

After running the pushover analysis with model 2, the first step consisted in the observation of the deformation distribution and evolution throughout the elements. The high lateral forces applied at the soft storey level have led to large demands of deformation capacity in the column and beam elements in that vicinity. In contrast, all remaining RC elements are kept practically un-deformed, without significant stresses, even for considerable top displacements (higher that 10 cm). The only masonry elements that were subjected to significant axial force increments are placed above and below the soft-storey, never reaching, however, the cracking strength for the same extreme top displacements values.

The point in the capacity curve of model 2 from which the structural system would continue to be represented was determined comparing the degradation of the reinforced concrete frames of model 1 (at the onset of the soft-storey mechanism) with the progressive degradation of the same components of model 2. There is a value of the base shear (marked with ▲ in the 2nd capacity curve of Figure 8) for which the deformation of the RC elements adjacent to the soft storey is reasonably similar to that of model 1 at the onset of soft storey mechanism (Figure 7). This is the stage beyond which the final capacity curve of the structure should follow the capacity curve of model 2. It is clear that there is a significant number of differences between these two stages, making these two not totally “compatible”.

Nevertheless, damage in the RC elements neighbouring the 3rd storey was by far considered the most important similarity to account for with care. In fact, the deformation of the RC concrete elements outside the 3rd storey is not crucial, since these are not subjected to subsequent high demands – i.e., the lateral displacement, after the soft-storey, is mainly due to the deformation of the columns and beams of this level. In what concerns the masonry, the most notorious discrepancy between the two compared stages are the several panels that had achieved the cracking strength in model 1 but that were modelled with the initial stiffness in model 2. This inconsistency can be, however, disregarded because the assumed post-cracking stiffness is almost identical to the initial one (see Figure 5). The key task left is precisely to find out whether the stress increment in the masonry elements of the level above and below the soft-storey is enough to cause their collapse (and consequently lead to new soft-storey formation) before the performance point is attained.

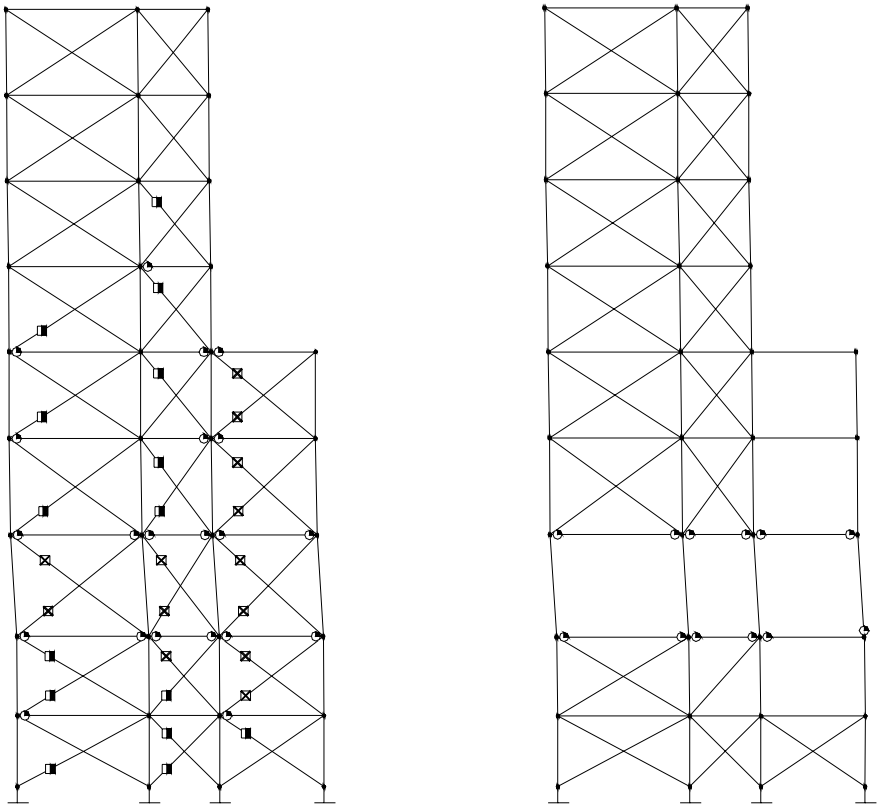

Model 1 **Model 2**

Figure 7: Comparison of the "equivalent" stage between Model 1 and Model 2 (for damage symbols refer to Figure 5).

The final capacity curve is obtained combining the first part of the capacity curve of model 1 (represented by a continuous line in Figure 8, before mark ○) with the second part of the capacity curve of model 2 (represented by a continuous line in Figure 8, after mark ▲). The result can be observed in the diagram shown on the right of Figure 8.

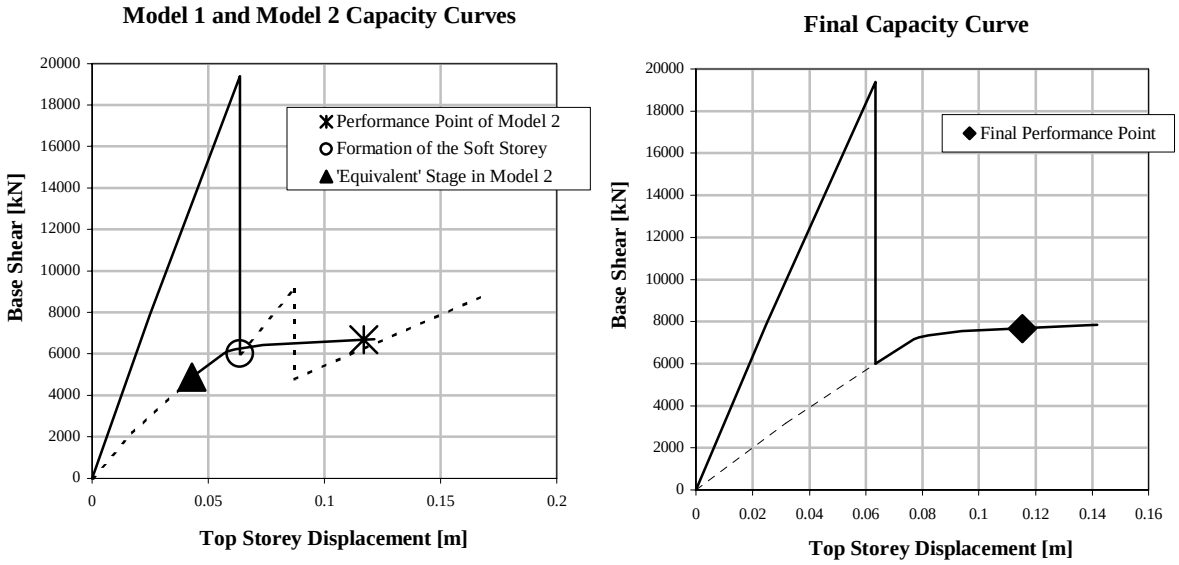

Figure 8: Capacity curve for each model and combination for final capacity curve.

Using all this information, it was then possible to compute the demand, for which the steps indicated in Procedure A of ATC, Applied Technology Council [4], were followed. The performance point (PP) resulting of this method is, in spectral coordinates, (0.264 g; 0.087 m) which, in terms of base shear *vs* roof displacement represents a demand of (7679.98 kN; 0.1153 m). The value of the base shear is composed of 6007.08 kN of model 1 and only 1672.9 kN of model 2. It should be noted that the equivalent viscous damping is 13.88 %, for a period that has lengthened from an initial value of 0.488 s to 1.153 s.

After the determination of the PP, it is possible to make the reverse conversion and identify the top displacement of model 2 that corresponds to the PP. A detailed analysis of the stress increment and deformation development in the masonry elements of model 2 was carried out for the loading stages in the capacity curve of model #2, until the estimated roof displacement value. The main conclusion is that the observed stress increments in the truss elements will not lead to the formation of another soft storey. Plastic hinge formation at PP can be observed in Figure 9, which was assembled from results of model 1 (for concrete elements outside the soft-storey and masonry) and model 2 (for concrete elements adjacent to the soft-storey).

As can be seen from Figure 9, although the risk of life-threatening injury is not negligible, some margin against total or partial structural collapse remains. Figure 9 also shows the storey shear distribution for the calculated demand.

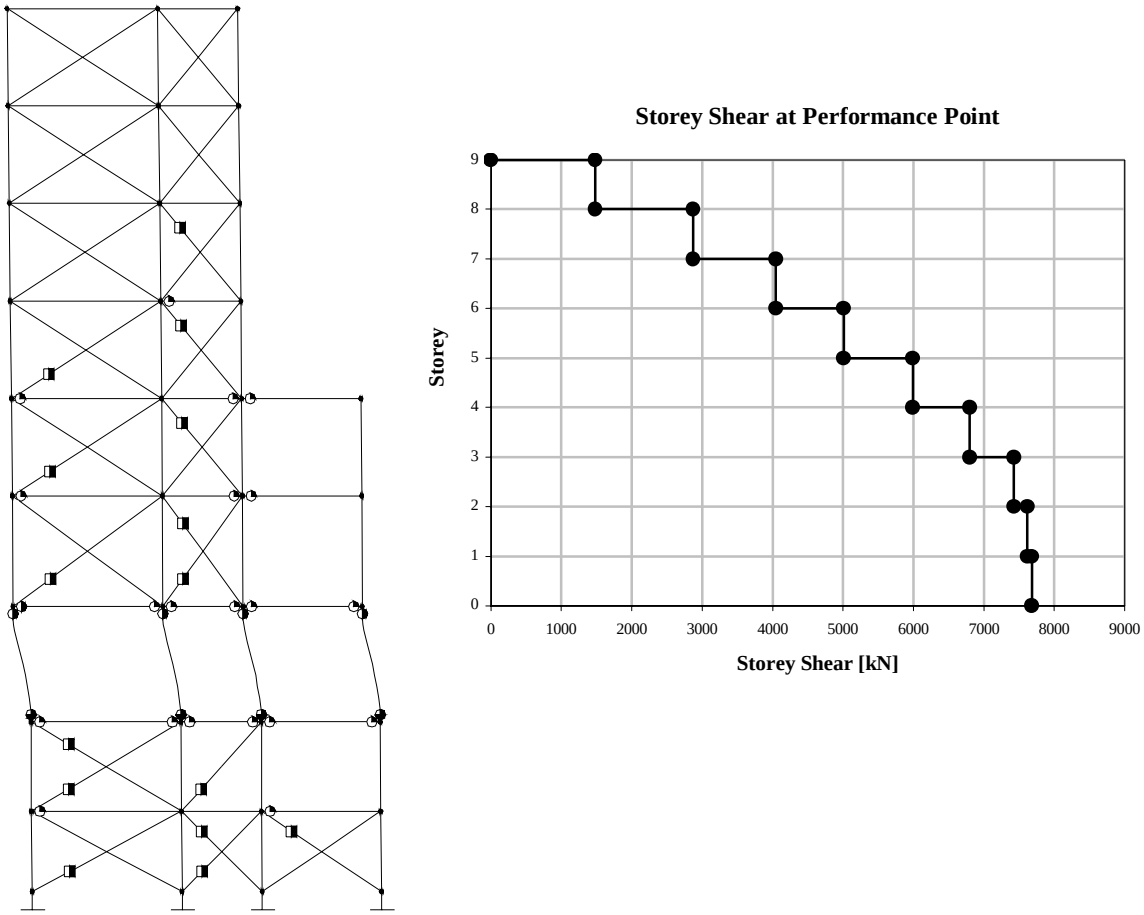

Figure 9: Expected damage description for concrete and masonry at performance point and storey shear (for damage symbols refer to Figure 5).

Preliminary Conclusions

Considerable engineering judgement has to be employed before linking base shear *vs* roof displacement curves "vertically", as presented in ATC, Applied Technology Council [4]. In fact, for small strength losses, the determination of the performance point can be uniquely based in the capacity curve of a single model including components influencing structural response at or near the performance point. On the other hand, high strength losses should be dealt with special care before progressing with the analysis. Sometimes, simple additional models have necessarily to be developed, as the one referred to as model 2, for a more precise structural characterization or, at least, for the validation of assumed hypothesis.

NON-STRUCTURAL VULNERABILITY ASSESSMENT

Pan-American Health Organization [8] presents guidelines for the seismic vulnerability of non-structural components, such as basic installations, equipment and architectural elements.

Basic installations and equipment elements are generally treated in the same way, classifying these in terms of the inherent vulnerability and the consequences of failure or malfunction of the element.

PAHO recommendations lead to a priorization of the hazard mitigation operations, computed as a weighing of the component vulnerability and of the consequences of its disruption or failure. PAHO

considers three degrees of component vulnerability (Low, Moderate and High), similarly to what happens with the severity of the consequences. The priorization is computed based on following priorities matrix shown in Table 1 (note: to a lower value corresponds a more urgent hazard mitigation operation).

Table 1: Priorities matrix, Pan-American Health Organization [8].

Vulnerability	Consequences		
	High	Medium	Low
High	1	4	7
Medium	2	5	8
Low	3	6	9

The implementation of the PAHO methodology led to the following list of interventions that are more urgent (priority lower or equal to 3): high voltage transformers (can tilt or tip, compromising the electrical power supply); lifts (un-braced closets that host the electrical relay components placed on the roof); suspended surgery lights (*pantof*) in the surgery room; and water lifelines (distribution ring at the 9th storey and roof tanks).

The most important architectural components are the walls, either external, non load-bearing or internal partition walls. These components are displacement-sensitive (in contrast with acceleration sensitive components, such as heavy medical equipment) and their integrity depends on the foreseeable interstorey drift. Serviceability and ultimate limit state drift values were estimated as being, respectively, of 0,125%-0,40 % and 0,4%-0,8%. The performance point estimated through non-linear static analysis for building block #22 corresponded to interstorey drift values lower than 0,18%, with the exception of the soft storey, where it reached 1,67%, clearly in excess of the ULS values.

CONCLUSIONS

The seismic vulnerability assessment study carried out in the Santa Maria Hospital expresses the expected structural and non-structural seismic performance, and point to damage reduction guidelines, aimed at the improvement of the connections of some basic lifeline components and to the structural seismic retrofit strategy.

Structural seismic vulnerability assessment of existing structures can greatly benefit from preliminary modal identification stages that can show unexpected strength and stiffness contribution of secondary structural or non-structural components. In the particular case of early RC structures, strong masonry walls, either facade or partition walls, have a significant stiffening effect that greatly determines the early nonlinear stages and can, as was the case, lead to a sudden drop of strength (and stiffness). From this stage on, damage tends to concentrate in-between two particular storeys, leading to an incipient soft storey mechanism. The structural behaviour changes to such an extent after the onset of the soft storey mechanism that a new “damaged” nonlinear model has to be developed. The results obtained in building block #22 have shown that, although collapse is not eminent, there is a large possibility of extreme damage concentration between two particular storeys, leading to high localized interstorey drift demands that could undermine the Hospital’s functionality.

Non-structural seismic vulnerability assessment led to a priorization of hazard reduction operations in terms of the basic installations and equipment.

ACKNOWLEDGEMENTS

The authors wish to express their gratitude to DGIES – Direcção Geral de Instalações e Equipamentos de Saúde – as a whole, and Mr. Virgílio Augusto, in particular, for having so successfully pursued the implementation of the present project. The Hospital staff contribution is also acknowledged by the authors. The help of Mr. Sebastião Falcão and the former work performed by Mrs. Patrícia Ferreira proved invaluable for the development of the present study.

REFERENCES

1. Oliveira, CS, Proença, J, Almeida, JP, Ferreira, P. “Programa de Avaliação da Vulnerabilidade Sísmica das Instalações Hospitalares da Área Metropolitana de Lisboa: Estudo-Piloto do Hospital de Santa Maria.” (in Portuguese) Technical Report ICIST EP Nº 25/03, 2003.
2. Computers and Structures Inc. “SAP2000 NonLinear Version 7.42: Structural Analysis Program.” Berkeley, California, 2001.
3. MHOPT “Regulamento de Segurança e Acções para Estruturas de Edifícios e Pontes.” (in Portuguese), 1983.
4. Applied Technology Council “Seismic Evaluation and retrofit of concrete buildings - Report ATC-40.” California Seismic Safety Commission, California, 1996.
5. Building Seismic Safety Council “NEHRP Guidelines for the Seismic Rehabilitation of Buildings.” Federal Emergency Management Agency, 1997.
6. Pires F. “Influência das Paredes de Alvenaria no Comportamento de Estruturas Reticuladas de Betão Armado Sujeitas a Acções Horizontais.” (in Portuguese) Specialist Thesis, LNEC, Lisbon, 1990.
7. CEN “ENV1998-1-1:1994: EuroCode 8 - Design and provisions for earthquake resistance of structures.” Brussels.
8. Pan-American Health Organization (Organización Panamericana de la Salud) “Fundamentos para la mitigación de desastres en establecimientos de salud.” OMS, 2000.
9. Newmark N, Hall W. “Earthquake Spectra and Design.“ Engineering monographs on earthquake criteria, structural design and strong motion records. EERI, Earthquake Engineering Research Institute, 1982: Vol. 3.